TUDelft

Delft University of Technology

A new generation of sloshing pressure sensors

Schreier, Sebastian; Poelma, Christian

Publication date
2018
Document Version
Final published version
Published in
Proceedings of the 28th (2018) International Ocean and Polar Engineering Conference (ISOPE-2018)

Important note
To cite this publication, please use the final published version (if applicable).
Please check the document version above.

A New Generation of Sloshing Pressure Sensors

Sebastian Schreier and Christian Poelma
Faculty 3mE, Delft University of Technology
Delft, The Netherlands

ABSTRACT

Sloshing impacts are highly dynamic and localized events. One problem in the measurement of sloshing impact pressures is the limited spatial resolution that can be achieved with current sensors. To overcome this hurdle a project was started to develop new sensors that allow to increase the spatial resolution of pressure measurements by a factor 5 compared to current test setups in sloshing experiments. The sensors were based on commercially available MEMS devices, which are suitable for measurements with liquid media. The main application of these devices are static pressure measurements. Therefore a qualification program for the new sensors for sloshing applications was started. First static and dynamic measurements in air gave promising results and encourage to continue this development with future tests in water.

KEY WORDS: Sloshing; Impact Pressures; MEMS; Sensor Qualification; Experimental Testing.

INTRODUCTION

In experimental sloshing investigations at model scale commonly used pressure sensors have diameters in the range of 3 mm to 6 mm and are arranged in clusters with spacing of order 10 mm (Loysel et al., 2012, Neugebauer et al., 2017, Ahn et al., 2013). Aim of sloshing experiments is mainly the assessment of tank design and cargo containment system of LNG cargo or fuel tanks. Therefore focus is mainly on extreme pressures. Dematteo and Ratouis (2013) indicated that with current sensor clusters higher impact pressures are likely missed between individual sensors. More recently spatial variability of impact pressures due to free surface instabilities during impact gained more attention (Frihat et al., 2016). While the instabilities can be observed by optical means, measurement of corresponding spatial pressure fluctuations is almost impossible with existing sensor arrangements.

Therefore this project was launched to develop new pressure sensor clusters with drastically improved spatial resolution. Very small pressure sensors are commercially available for OEM applications e.g. in automation. These are semiconductor Micro Electric Mechanical Systems (MEMS) used mainly for static and slowly varying pressures. Furthermore these MEMS are bulk electronic devices that require external micro-electronic wiring and packing to become useful sensors. First specimen of such sensors were recently assembled and tested in air. Observations and results are reported in this paper.

EQUIPMENT AND SETUP

MEMS Pressure Sensors

The pressure sensing devices selected for this project were EPCOS C32 industrial with absolute pressure range of 1.6 bar, in-plane dimensions of 1.7 mm by 1.7 mm, and a vacuum reference cavity at their back. These were piezoresistive semiconductor dies based on the working principle of a Wheatstone bridge. Typical sensitivity of these devices was given as 70 mV/bar at excitation voltage of 5 V. Non-linearity was specified as 0.3 % of the measuring range. Hydraulics and pneumatics in industry and automotive were their intended fields of application. Working media were specified as non-aggressive gases and liquids. Wiring to external circuitry was required by gold wire bonding (EPCOS, 2009).

From the mentioned fields of application it was concluded that the selected sensor dies were mainly intended for measurement of static and slowly varying pressures. Unfortunately no information on the dynamic properties like response time or natural frequency of the sensor dies was available. With working media specified as non-aggressive gases and liquids these sensor dies were deemed suitable for measurements in water. Based on their piezoresistive working principle and configuration for absolute pressure measurement these sensor dies would measure the sum of atmospheric pressure, static water pressure and dynamic impact pressures. This required a large dynamic range of the data acquisition system as detailed below. The sensors were mainly selected for their small size and the tests reported here were carried out as a first step into a full qualification program for dynamic measurements.

For the first tests the sensor dies were glued and wire-bonded to printed circuit boards at the Else Kooi Lab of EEMCS Faculty, TU Delft. Arrangements chosen were single sensors and 5 sensors in one line, see Figs. 1 and 2. For testing purposes 2 versions of in-line sensor arrangements were produced, one with spacing s =1.0 mm and one with s = 1.5 mm. A hole in the circuit board underneath each sensor die allowed pressure access to the pressure port on the underside of the

sensors. The 5 sensor arrangement called Pressure Sensor Cluster 5 (PSC5) was used for testing in this project. Individual sensors are identified as PSC5-1 through PSC5-5.
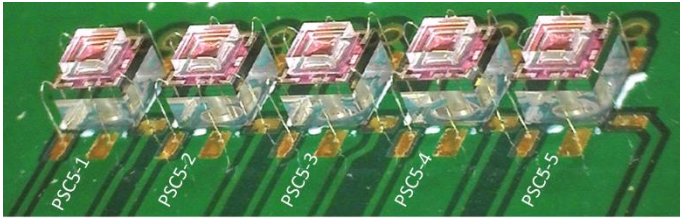
Fig. 1. Pressure sensor dies mounted on printed circuit board. Picture by Henk van Zeijl, TU Delft.

As can be seen from Fig. 1 the bonding wires for 4-wire connection to the data acquisition system were very delicately arranged on the sensor dies. For testing purposes sensors were not covered by protective molding compound, which otherwise is common practice with wire-bonded devices. Accordingly, at this stage the sensors were only tested in air. Waterproofing of the sensor wiring and its possible influence on the sensor properties will be addressed in the near future.
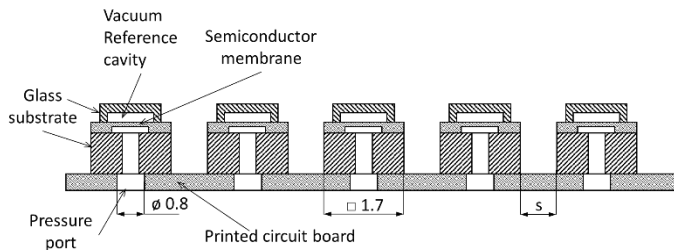
Fig. 2. Schematic elevation of a pressure sensor cluster, not to scale. Dimensions in mm.

Reference Sensor and Data Acquisition System

The reference pressure sensor was a model PDCR 42 with a range of 10 psi (0.690 bar) gauge pressure of Druck Ltd. The sensing element of this sensor was a Wheatstone bridge with 4-wire connection and a nominal sensitivity of 50 mV full range at 12 V excitation voltage. This gave the nominal calibration factor of $F_n = 0.1656$ bar/(mV/V).

Data acquisition system for this campaign was National Instruments Chassis NI PXIe-1078 equipped with NI PXIe-8840 Quad-Core processor and NI PXIe-4331 8-Channel 24 bit bridge analogue input card. Internal excitation voltage of $U_e = 2.5$ VDC was used for all sensors. Sampling rate was set to $f_s = 100$ Hz for reference sensor calibration and to $f_s = 10$ kHz for measurements with PSC5 involved. At each of these sampling rate settings the PXIe-4331 input card used an internal anti-aliasing filter with low-pass frequency $f_a = 0.4\ f_s$ (National Instruments, 2010).

Test setup

Testing was carried out in three steps. First the reference pressure sensor was statically calibrated using a water column as external reference. Second the pressure sensor cluster was tested in air with some dynamic pressure pulses. Third the PSC5 was statically calibrated against the reference pressure sensor. The sequence of dynamically testing the PSC5 before calibration was chosen because of the delicacy of the sensor

wiring and the chance of breaking the bonding wires in the calibration setup.

Setups for static calibration of the reference pressure sensor and the PSC5 is shown in Fig. 3. On the left-hand side of Fig. 3 the setup for calibration of the reference sensor is depicted. The reference sensor was connected to a sealed section of horizontal pipe via valve V_1. The pipe was partially filled with water. It was pressurized by a connection to a water tap via valve V_2 and drained via valve V_4. To build up the pressure in a controlled manner a transparent hose with a vertical section was also connected to the pipe via valve V_3. The upper end of the hose was open to atmospheric pressure p_{atm}. The water column height h in the transparent hose with respect to the initial water level in the pipe section was used to determine the pressure at the reference pressure sensor. The change of water level in the pipe due to air compressibility was neglected.

The right-hand side of Fig. 3 depicts the setup for calibration of the pressure sensor cluster. A pressure housing containing the PSC5 was connected to the horizontal pipe section of the test setup by valve V_5. The reference sensor PDCR was moved from its calibration position to the top of the pressure housing. The pressure housing was filled with air. Due to the larger air volume in the test setup the variation in water level with increasing pressure was larger. Therefore the PSC5 was calibrated against the reference sensor and the water column in the hose was only used to set the pressure.
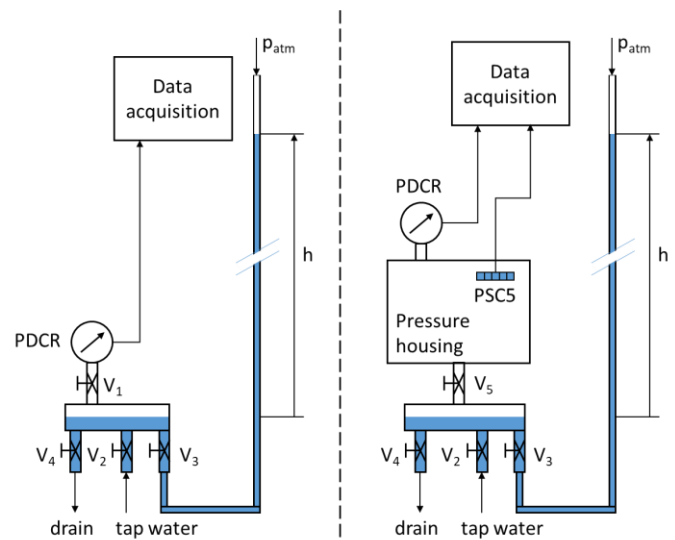
Fig. 3. Calibration test setups. Static calibration of reference sensor PDCR (left), calibration of pressure sensor cluster (PSC5) against reference sensor PDCR (right).

STATIC MEASUREMENTS

Reference Sensor Calibration

For calibration of the reference sensor the signal of the sensor was continuously measured with valves V_1 and V_3 open, while the water column height was adjusted in steps using valves V_2 and V_4.

The nominal calibration factor was used to convert the measured signal into a pressure value to have an indication of the current pressure value. The resulting curve is presented in Fig. 4. Here clearly the steps in pressure can be distinguished. The overshoots and undershoots at the

transitions between the steps were due to the water column in the hose and the air in the pipe section forming a dynamic system, which needed to settle to its new equilibrium point.
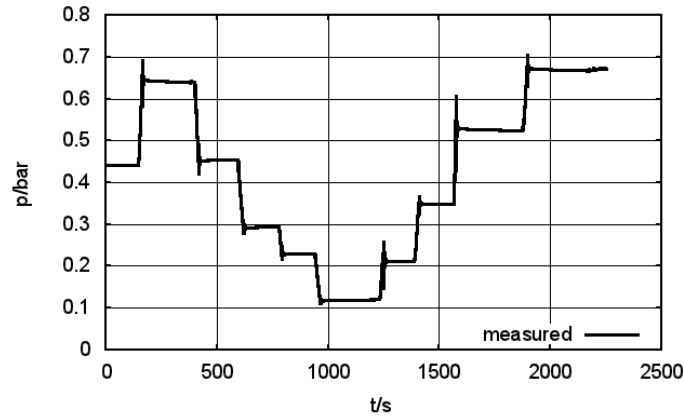
Fig. 4. Measured signal during reference sensor calibration.

From the plateaus of the measured pressure data 10 sections of 30 seconds with stationary pressure signal were selected. Over each section the mean value p_m of the measured data was computed as well as the standard deviation σ of the pressure data. The resulting data is summarized in Tab. 1. The mean pressures p_m were then converted back to the measured voltage signal U_{sig} by dividing the pressure by the nominal calibration factor F_n. Furthermore the pressure p_{wc} due to the water column height h was calculated according to equation (1) with the water density of $\rho = 998 \frac{kg}{m^3}$ and the gravitational acceleration $g = 9.81 \frac{m}{s^2}$.

$$p_{wc} = \rho g h \tag{1}$$

Tab. 1. Sectional data for reference sensor calibration.

section no.	h/m	p_m/bar	σ/bar	U_{sig}/ (mV/V)	p_{wc}/bar
1	5.245	0.4420	2.63E-05	2.669	0.5135
2	7.263	0.6406	1.18E-04	3.869	0.7111
3	5.362	0.4539	5.34E-05	2.741	0.5250
4	3.740	0.2938	7.23E-05	1.774	0.3662
5	3.093	0.2301	8.42E-05	1.389	0.3028
6	1.961	0.1188	9.74E-05	0.718	0.1920
7	2.900	0.2111	2.17E-05	1.275	0.2839
8	4.288	0.3474	5.70E-05	2.098	0.4198
9	6.104	0.5267	1.71E-04	3.180	0.5976
10	7.540	0.6680	9.42E-05	4.034	0.7382

From the last two columns of Tab. 1 the new calibration factor F_{ref} of the reference pressure sensor was computed as the slope of the linear regression along with the offset p_0 from the intercept. To qualify the calibration the correlation coefficient R^2 as well as the RMS value of the difference between the regression line and the measured values normalized by the full scale value of the sensor according to equation (2) were computed. The results are summarized in Tab. 2. Fig. 5 shows the regression line with the measured data.

$$RMS = \sqrt{\frac{\sum_N \left(U_{sig,i} \cdot F_{ref} + p_0 - p_{wc,i}\right)^2}{N}} \tag{2}$$

Tab. 2. Calibration data of the reference pressure sensor.

F_{ref}/(bar/(mV/V))	p_0/bar	R^2	RMS/FS
0.1647	0.073987	0.999999	0.026%
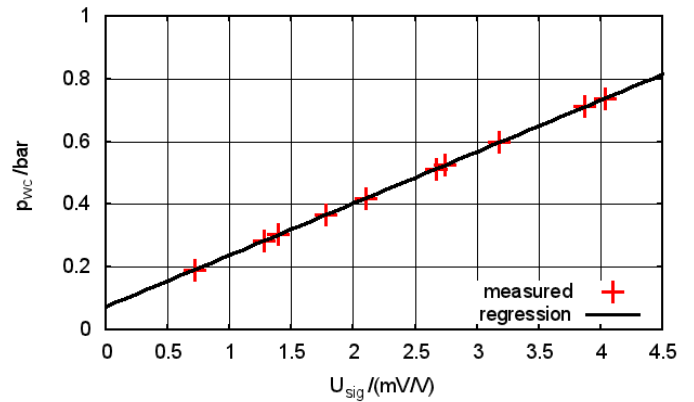
Fig. 5. Regression line and measured data points for the reference pressure sensor.

Fig. 5 and Tab. 2 indicate the excellent linearity of the reference sensor. The new calibration factor F_{ref} was used for the calibration of the pressure sensor cluster.

Pressure Sensor Cluster Calibration

For the calibration of the pressure sensor cluster data was recorded from the PSC5 and reference pressure sensor in the pressure housing. During the mounting of the sensors and closing the pressure housing all valves were closed. Then the measurement was started and after some time the valve V_5 connecting the pressure housing with the pipe section was opened. This was marked by the first pressure drop seen in Fig. 6. After several more seconds valve V_3 connecting the hose to the pipe section was opened. This was again marked by a pressure drop, this time followed by oscillations due to the water column settling to its new equilibrium condition. With valves V_3 and V_5 open the pressure in the system was increased stepwise by using valve V_2.

After a preliminary check of the data the recorded signals were first low-pass filtered using a 2nd-order Bessel filter with a cut-off frequency of 10 Hz and consecutively resampled at 50 Hz to reduce the amount of data to process. Furthermore the starting offset of all pressure signals was removed. The resulting time traces based on nominal calibration factors for the PSC5 sensors are shown in Fig. 6. Only four lines of the five PSC5 sensors are shown because sensor PSC5-5 did not work due to a broken cable.
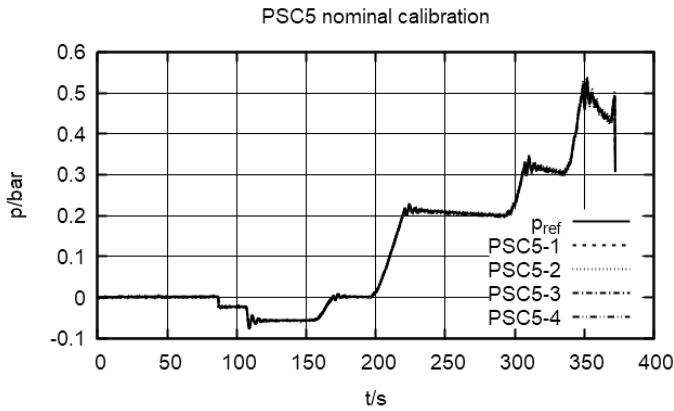
Fig. 6. Time series of PSC data and reference pressure before calibration of PSC sensors.

Due to a leak in the pressure housing the pressure constantly dropped. The dropping rate increased with a higher pressure level. Therefore the calibration data was gathered from 5 sections each of 10 seconds duration from the plateaus between 90 s and 340 s of the time series. Per PSC5 sensor and for the reference sensor the pressure was averaged over the section length of 10 seconds. Using the nominal calibration factor of the PSC5 sensors of $F_{PSC5,n} = 0.07$ bar/(mV/V) the averaged pressure values were converted back to the voltage signals. These voltage signals were then plotted against the reference pressure. The data points along with the regression lines are shown in Fig. 7 for the individual PSC5 sensors.

All four operational PSC5 sensors showed a very good linear behavior. The results from linear regression are summarized in Tab. 3. Here again the deviation of the data points from the regression line was expressed by the RMS value calculated with the individual calibration factors $F_{PSC5,i}$ according to equation (2) and normalized by the achieved pressure range of $p_r = 0.3$ bar. For comparison with the nominal sensitivity of the sensors the sensitivity is given for the reference condition with an excitation voltage of $U_e = 5$ VDC.

Tab. 3. Calibration data of the four PSC5 sensors.

No.	$F_{PSC5,i}$/ bar/(mV/V)	$p_{0,i}$/bar	R^2	RMS/p_r	sensitivity @ 5 V in mV/bar
PSC1	0.06845	0.0006636	0.999993	0.12%	73.04
PSC2	0.06919	0.0009106	0.999994	0.12%	72.26
PSC3	0.07063	0.0014221	0.999995	0.10%	70.79
PSC4	0.06832	0.0009592	0.999994	0.11%	73.18

When the data obtained from the PSC sensors was recalibrated using the new calibration factors also the slight discrepancies between the curves vanished and all five curves perfectly overlapped as can be seen in Fig. 8.
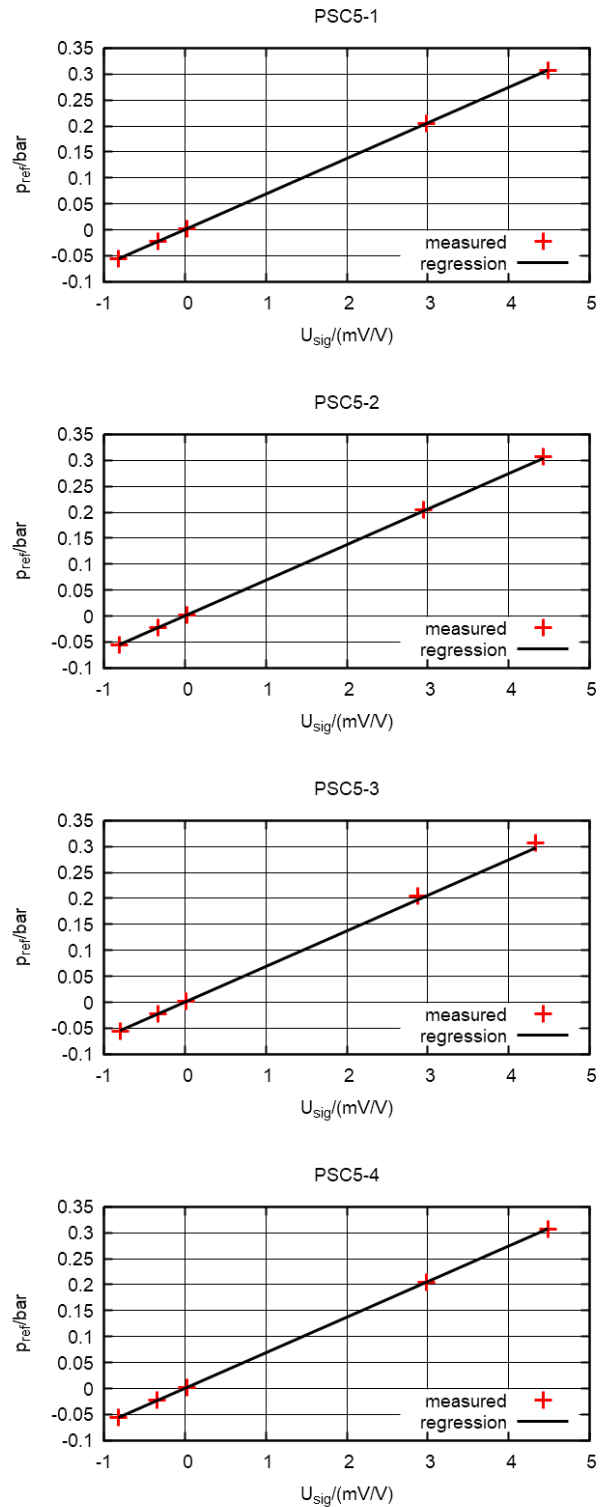
Fig. 7. Calibration lines of the four operational PSC5 sensors.
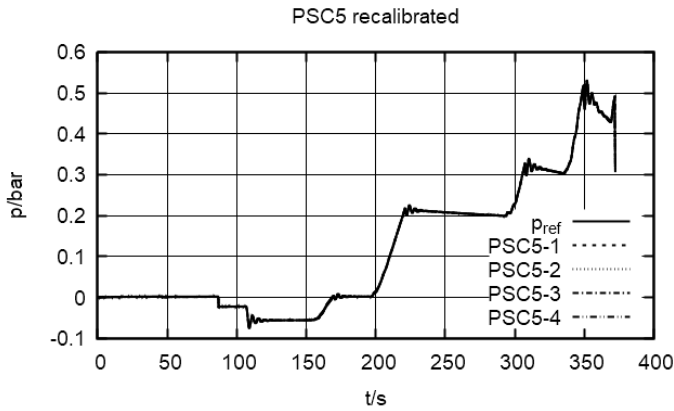
Fig. 8. Time series of PSC5 data and reference pressure after calibration of PSC5 sensors.

DYNAMIC MEASUREMENTS

In order to obtain a first insight in the dynamic measurement capabilities of the PSC5 sensors some very crude tests were carried out in air. As mentioned before these measurement were taken before the calibration of the PSC sensors. The data presented in the following figures was recalibrated afterwards and any offset removed. These tests were carried out without the reference sensor present. Therefore the results shown here are purely indicative.

The first dynamic test was conducted by snapping a finger at a distance D of approximately 5 cm from the PSC5 sensor. A sketch of the setup is given in Fig. 9. The PSC5 was mounted in a protective housing with the pressure ports of the printed circuit board facing up. The mark (x) in the sketch indicates the position of the snapping fingers with respect to the sensors.
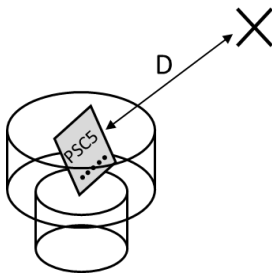
Fig. 9. Sketch of setup for dynamic tests. Mark (x) denotes approximate position of sound source.

The finger was snapped at the sensor multiple times with a separation of several seconds. Four representative pressure time series are presented in Figs. 10~13. All four repetitions showed oscillating signals by all four operating sensors where the oscillations were always in phase with each other and of roughly the same amplitude for a single repetition. For the first two repetitions of Figs. 10 and 11 the oscillation period of the pressure was 0.5 ms. This was determined from the first 4 oscillations, which were completed in 2 ms. Thus the oscillation frequency is 2 kHz. For the repetitions shown in Figs. 12 and 13 the oscillation frequency was slightly higher.

A very positive finding from these crude dynamic tests was the low noise level on the signals considering that the signals discussed here were at a level of 1/1000 and below of the sensors' full scale range.
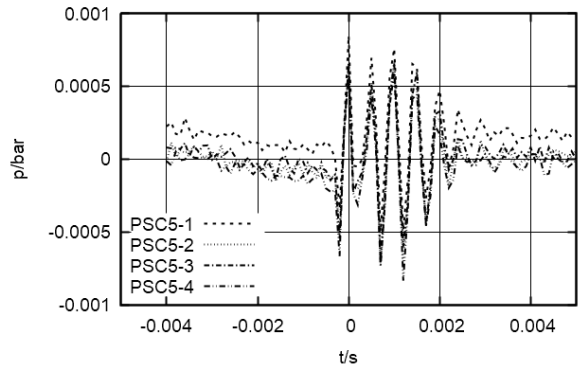
Fig. 10. PSC5 pressure time series of first snapping sound.
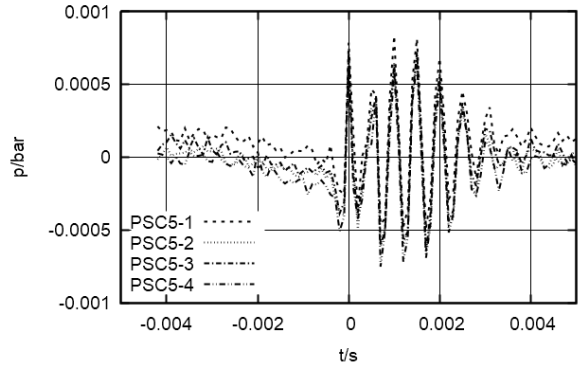
Fig. 11. PSC5 pressure time series of second snapping sound.
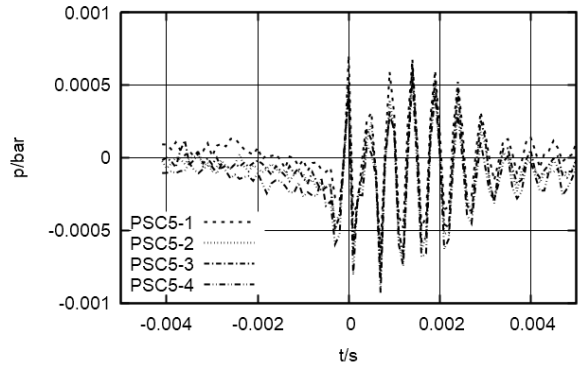
Fig. 12. PSC5 pressure time series of third snapping sound.
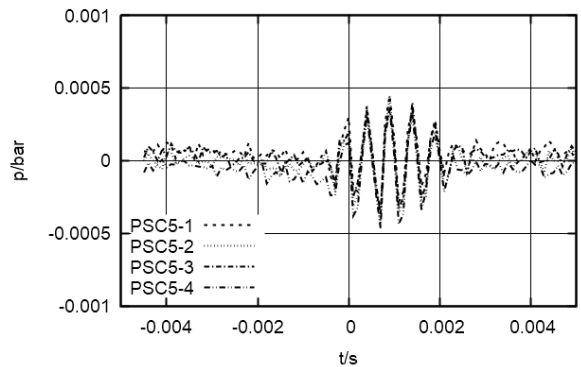
Fig. 13. PSC5 pressure time series of fourth snapping sound.

For the second dynamic test a popping sound was made by suddenly opening the mouth, again approximately 5 cm away from the sensors with the same setup as given in Fig. 9. Also this test was repeated several times. Representative pressure time series of two repetitions are presented in Figs. 14 and 15.
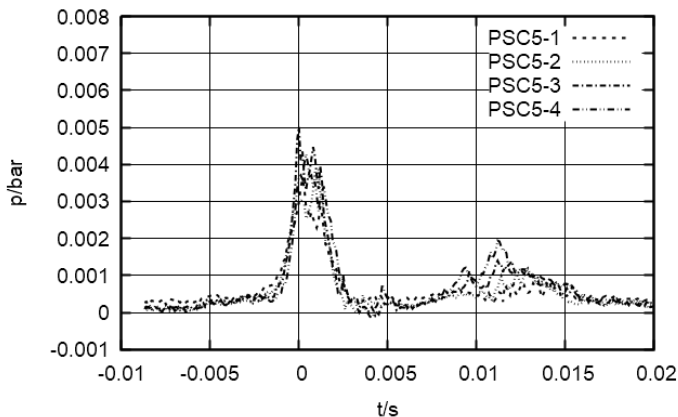
Fig. 14. PSC5 pressure time series of first popping sound.
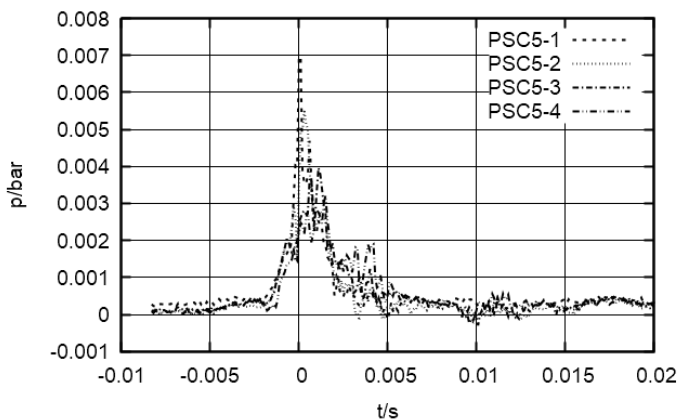
Fig. 15. PSC5 pressure time series of second popping sound.

As visible in both Figs. 14 and 15 all four operational sensors reacted to the popping sound by a sharp increase in their signal, which then remained elevated for several milliseconds before the signals settled back to their starting values. It can also be seen that in the second repetition shown in Fig. 15 sensors PSC5-1 and PSC5-2 exhibited a sharper increase in signal compared to sensors PSC5-3 and PSC5-4, whereas in the first repetition of Fig. 14 all four sensors reacted more evenly. Given the nature of the test setup no further interpretation of the signals is attempted here.

DISCUSSION

The calibration of the PSC5 sensors confirmed the very good linearity that was expected from these industrial sensors. Furthermore also the new sensitivity values were well within the range specified by the manufacturer. Therefore these calibrations are deemed reliable.

On the other hand the calibration was hampered by the leak in the pressure housing. By simultaneously measuring the pressure signals of the PSC5 sensors and the reference sensor the influence of the non-stationary pressure was compensated.

The oscillation frequency observed in the dynamic measurements revealed that the sampling rate of 10 kHz was chosen too low for these tests to obtain reliable data on the magnitude of the pressure.

CONCLUSIONS

In this project the first steps were taken towards a new generation of pressure sensors for sloshing and other impact applications. The mounting of the sensors on printed circuit boards was successful and first static as well as dynamic measurements in air could be conducted. The measurement results led to the following conclusions.

- The selected pressure sensor dies showed very good linearity in the calibration.
- The response to first dynamic excitations of the sensors were plausible.
- The dynamic response of the sensor dies requires further investigation with sampling rates higher than 10 kHz.

With these results the next steps of this project will be the protection of the delicate bonding wires to make the PSC5 sensors more robust and also suitable for testing in water. Thereafter a complete qualification program for these sensors needs to be designed and executed with due consideration of dynamic sensor behavior.

ACKNOWLEDGEMENTS

REFERENCES

Ahn, Y, Kim, KH, Kim, SY, Lee, SW, Kim, Y, and Lee, JH (2013). "Experimental Study on the Effects of Pressure Sensors and Time Window in Violent Sloshing Pressure Measurement," *Proc 23rd Int Offshore and Polar Eng Conf*, Anchorage, Alaska, USA, ISOPE, 3, 186-193.

Dematteo, A, and Ratouis, A (2013). "Stochastic Simulation of the Pressure Field Induced by Sloshing Impacts," *Proc 23rd Int Offshore and Polar Eng Conf*, Anchorage, Alaska, USA, ISOPE, 3, 290-297.

EPCOS AG (2009). "C32 Product Brief", http://www.texim-europe.com/promotion/449/pressure%20sensor%20c32_products%20brief_te.pdf, 05.03.2018.

Frihat, M, Karimi MR, Brosset, L, Ghidaglia, J-M (2016). "Variability of impact pressures induced by sloshing investigated through the concept of "singularization"," *Proc 26th Int Offshore and Polar Eng Conf*, Rhodes, Greece, ISOPE, 3, 901-914.

Loysel, T, Chollet, S, Gervaise, E, Brosset, L, and De Seze, P-E (2012). "Results of the First Sloshing Model Test Benchmark," *Proc 22nd Int Offshore and Polar Eng Conf*, Rhodes, Greece, ISOPE, 3, 398-408.

National Instruments Corporation (2010). "NI PXIe-4330/4331 Specifications".

Neugebauer, J, Liu, S, Potthoff, R, and el Moctar, O (2017). "Investigation of the Motion Accuracy Influence on Sloshing Model Test Results," *Proc 27th Int Offshore and Polar Eng Conf*, San Francisco, California, USA, ISOPE, 3, 1054-1061.